20th International Conference on Structural Mechanics in Reactor Technology (SMiRT 20)
Espoo, Finland, August 9-14, 2009
SMiRT 20-Division Ⅱ Fracture Mechanics and Structural Integrity, Paper 2531

Evaluation on the Fracture Properties of Heated Concrete by Using Poly-linear Tension Softening Inverse Analysis

Yoshinori Kitsutaka[a] and Koichi Matsuzawa[b]

[a]*Department of Architecture and Building Engineering, Faculty of Urban Environmental Sciences, Tokyo Metropolitan University, Tokyo, Japan, E-mail: kitsu@tmu.ac.jp*
[b]*Tokyo Metropolitan University, Tokyo, Japan*

Keywords: Concrete, Fracture mechanics, Tension softening diagram, Fracture energy, Heating.

ABSTRACT

Concrete structures for nuclear power generation may be subjected to heating action for a long period. However, the fracture properties of concrete under the heating action are not yet clarified. Also the evaluation of the fracture parameter for inelastic materials is an important subject in the field of fracture mechanics of concrete. This paper reports on the investigation into the fracture properties of concrete subjected to the effects of heating condition for 60℃ by using the poly-linear tension softening inverse analysis.

Poly-linear approximation method for calculating the tension softening diagram from a load-displacement curve based on the stepped inverse analysis was introduced. In this method, the nonlinear crack equation was solved by an iteration program for evaluating the optimum softening inclinations of the tension softening diagram. From the test and analysis, specimen of maximum aggregate size 10 mm tends to show high energy consumption to compare with specimen of maximum aggregate size 5 mm and specimens of maximum aggregate size 5 mm cured at 60℃ tend to develop lower fracture energy than those cured at 20℃.

1. INTRODUCTION

Concrete structures for nuclear power generation may be subjected to heating action for a long period. Many studies have already reported that the strength of concrete subjected to heating can be retained by maintaining temperature conditions of not more than around 65℃ under general control standards for nuclear power generation. The effect of the heating should be considered to discuss the long-term safety and the durability of concrete structures. However, the fracture properties of concrete under the heating action are not yet clarified.

On the other hand, evaluation of the fracture parameter for inelastic materials is an important subject in the field of fracture mechanics of concrete. Many researchers have attempted to apply linear or non-linear fracture mechanics to express the fracture behaviour of concrete. However, concrete manifests a softening behaviour and hence, is considered as an inelastic material. This behaviour is mainly due to the effect of a fracture process zone (FPZ) which is developed ahead of the crack tip. The existence of FPZ makes it difficult to specify not only the energy changes by fracturing but also the crack advance length of concrete.

It has been pointed out by many researchers that the tension softening diagram (TSD) is a very useful basic parameter characterizing the fracture behaviour of concrete. The tension softening diagram can also be used to estimate the energy changes in the fracture process zone, and it may give us a lot of information on the elastic-plastic fracture parameter. Several researchers have attempted to measure the tension softening diagram using direct tension tests (Gopalaratnam and Shah 1985; Wang et al. 1990). However, this requires a special testing machine and it is very difficult to obtain a stable loading condition during the test. Moreover, the direct tension test measures the average stress and not the accurate relationships of cohesive stress and crack opening. Roelfstra and Wittmann (1986) proposed the inverse analysis to determine the bi-linear tension softening diagram by means of the cohesive force model analysis and a fitting program. However, this can only be used to calculate the bi-linear type tension softening diagram. Li et al. (1987) presented an

experimental method to determine the tension softening diagram based on the J-integral concept. This method is a very simple one to calculate the tension softening diagram, but two specimens are needed for an analysis, and thus the results have a high variance without assuming the function of *J*-integral curve. The poly-linear tension softening inverse analysis was proposed by Kitsutaka et al. (1994, 1997) and this method was authorized for Japan Concrete Institute Standard (JCI-S-001-2003) as an appendix method of estimating tension softening curve of concrete.

In this study, the poly-linear tension softening inverse analysis method was introduced and the fracture properties of concrete subjected to the effects of heating condition for 60℃ were discussed.

2. POLY-LINEAR TENSION SOFTENING INVERSE ANALYSIS

2.1 Calculation of load displacement relationship by using poly-linear tension softening diagram

The tension softening diagram (TSD) is determined based on the cohesive force model (CFM) concept (Hillerborg 1976) as shown in Fig. 1. The Dugdale-Barenblatt-type TSD can be represented by a poly-linear line as shown in Fig. 2.

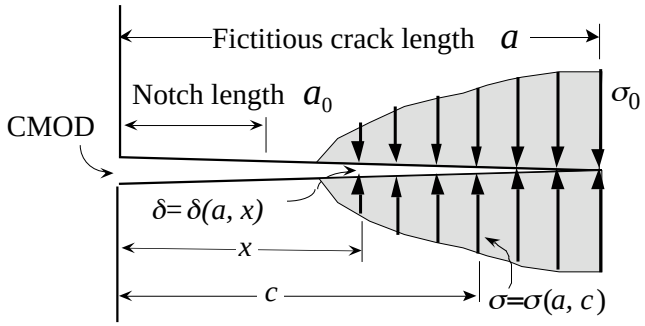

Figure 1. Cohesive force model

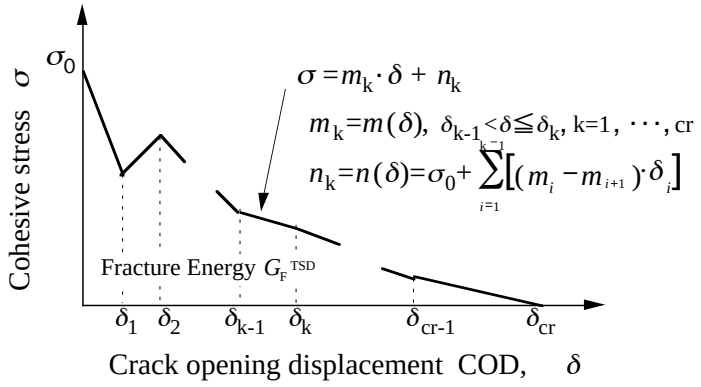

Figure 2. Poly-linear tension softening diagram (TSD)

The cohesive stress $\sigma(a,x)$ is the poly-linear function of crack opening displacement of $\delta(a, x)$;

$$\acute{o}(a,x) = m(\ddot{a}) \cdot \ddot{a} + n(\ddot{a}); \qquad \delta = \ddot{a}(a,x) \tag{1}$$

where a is the crack length, x is the point on the crack surface, m(δ) is the softening inclination (see Fig.1, 2); n(δ) is the inflection point which is a function of initial σ_0 and m(δ) as follows.

$$n(\ddot{a}) = \acute{o}_0 + \sum_{i=1}^{k-1} \left\{ \left[m(\ddot{a}_i) - m(\ddot{a}_{i+1}) \right] \cdot \ddot{a}_i \right\}, \quad \ddot{a}_{k-1} < \ddot{a} \le \ddot{a}_k, \; k = 1,\ldots,cr \tag{2}$$

Thus the TSD prediction problem is essentially the problem of obtaining appropriate σ_0 and $m(\delta)$. The boundary conditions of the cracked specimen with cohesive forces are provided by the equilibrium of stress intensity factor in (3) and the equilibrium of COD in (4) (Foote et al. 1986).

$$K(a) = K_p(a) + K_r(a) = 0; \qquad \ddot{a}(a,x) = \ddot{a}_p(a,x) + \ddot{a}_r(a,x) \tag{3,4}$$

where $K(a)$, $K_p(a)$, $K_r(a)$ are the stress intensity factors on the crack tip due to the total force, the external load and the cohesive stress, respectively, and $\delta_p(a, x)$, $\delta_r(a, x)$ are the CODs due to the external load and the cohesive stress, respectively. These relationships can be calculated by using FEM or BEM, but in the case of a simple beam, the solution can be obtained using the calculation results of linear fracture mechanics (Tada 1985). $K_p(a)$, $K_r(a)$ appeared in (3) are;

$$K_p(a) = \acute{o}_p \sqrt{\partial a} \cdot F(a,d) \tag{5}$$

$$K_r(a) = \frac{2}{\sqrt{\pi a}} \int_0^a \sigma(a,c) \cdot G(a,c,d)\,dc \tag{6}$$

Where, $\sigma_p$is the nominal stress due to the external load, d is the height of beam, c is the coordinate indicating the point on crack surface where cohesive force is acting (see Fig.1), and $F(a, d)$ and $G(a, c, d)$ are weight functions. For the calculation of COD, Castigliano's theorem is applied (Tada et al. 1985; Foote et al. 1986; Cotterell et al. 1992). Displacement of cracked body can be expressed by stress intensity factors (K-superposition method);

$$dy = d_0 + \frac{2}{E} \int_x^a K(z) \left[\frac{\partial K_F(z)}{\partial F} \right]_{F=0} dz \tag{7}$$

where dy is the displacement on x, d_0 is the displacement of uncracked body, z is the coordinate indicating the crack length for the integration, F is the fictitious force acting on the point x, E is the elastic modulus, $K(z)$ is the stress intensity factor producing the displacement dy, and $K_F(z)$ is the stress intensity factor due to fictitious force F acting for the direction of dy. Substituting (5) and (6) into (7) and calculating the left hand side of (4);

$$\delta_p(a,x) = \frac{4\sigma_p}{E} \int_x^a F(z,d) \cdot G(z,x,d)\,dz \tag{8}$$

$$\delta_r(a,x) = \frac{8}{\pi E} \int_0^a \sigma(a,c) \left[\int_x^a \frac{1}{z} G(z,x,d) \cdot G(z,c,d)\,dz \right] dc \tag{9}$$

Substituting (5) and (6) to (3), also (8) and (9) to (4), and canceling the σ_p appeared in (3) and (4), then the simple crack integral equation is obtained as (10). $H(a, x, c)$ is the weight function called the H-function, and it does not depend on the loading condition.

$$\delta(a,x) = \int_0^a \sigma(a,c) \cdot H(a,x,c)\,dc \tag{10}$$

$$H(a,x,c) = \frac{8}{\partial E} \int_x^a \left[\frac{1}{z} G(z,c,d) - \frac{1}{a} G(a,c,d) \frac{F(z,d)}{F(a,d)} \right] \cdot G(z,x,d)\,dz \tag{11}$$

Substituting $\sigma(a, x)$ of (1) into (10) and expressing in the matrix form for the total number of nodes (=n) on the crack surface, we obtain the simultaneous crack equation as follows;

$$\mathbf{A}_{ij}\mathbf{d}_i = \mathbf{b}_i\ ,\quad i,j = 1,...,n$$

where

$$\mathbf{A}_{ij} = -m_k \cdot l_j \cdot H(a,x_i,c_j) + \phi(i,j);\quad k = 1,...,cr;\quad \phi(i,j) = \begin{cases} 1, & i = j \\ 0, & i \neq j \end{cases} \tag{12}$$

$$\mathbf{d}_i = \ddot{a}(a,x_i)$$

$$\mathbf{b}_i = \sum_{j=1}^{n}\left[m_k \cdot l_j \cdot H(a,x_i,c_j)\right]$$

l_j is the width of the effective area of cohesive stress acting on node j. In the poly-linear TSD case, the coefficient of m_k is the function of the $\mathbf{d}_i$ as the solution of this simultaneous equation. This problem can be solved by performing several iterations, changing the appropriate k of m_k in each node after the calculation.

The load point displacement (LPD) is obtained from the accumulation of the displacement due to the external load and the displacement due to the cohesive stress. They can be calculated by the Castigliano's theorem by substituting (5) and (6) into (7) with considering the vertical load P as fictitious force of F (LLorca and Elices 1990).

2.2 Stepped inverse analysis of poly-linear tension softening diagram

The author has demonstrated the basic concept of analyzing the poly-linear TSD from a measured load displacement curve (Kitsutaka et al. 1994). Fig.3 shows the relationship between crack propagation and analyzed TSD which forms the basic concept of this analysis.

The softening inclination m_k and COD of node 1 at step k (δ_{k1}) were determined by optimizing the load calculated by a crack equation analysis to the load obtained by an experiment. In this step, former values of all m_k and δ_{k1}were fixed and they were used as the constitutive law for calculation. This method can be summarized by stating that the relationship between COD and cohesive stress on node 1 (the fixed point $x=a_0+0.5l_1$) is calculated considering the boundary conditions of all nodes for each step. Because of the monotonous increase of COD from a crack tip to a crack mouth, in the case of uniform materials, the COD of node 1 is the largest in every calculation, therefore the constitutive law for all CODs should exist for each step and optimum TSD should be obtained. Young's modulus E can be obtained from the initial inclination of load point displacement curve. σ_0 can be determined by analyzing the initial load point displacement curve temporary assuming the softening inclination to have the constant value of zero (Dugdale model).

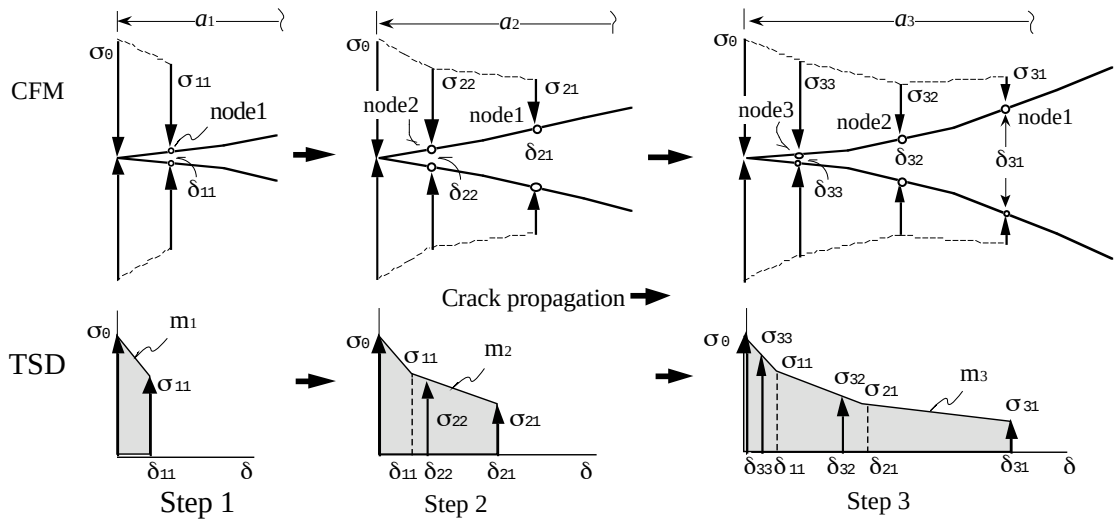

Figure 3. Concept of poly-linear tension softening diagram inverse analysis

2.3 Comparison of test result and analysis

Fig. 4 shows typical load-load point displacement (L-LPD) curves obtained three-point bending tests for center-notched beam specimens (specimen size, span length, and notch length were 100x100x450mm, 400mm, and 50mm). Specimens are a normal strength concrete specimen (NSC, compressive strength of 28 days is 45.3 MPa) and a high strength concrete specimen (HSC, compressive strength of 28 days is 99.7 MPa).

In Fig.4, for convenience, the TSD calculated from the L-LPD curve by the present analysis method is also shown. The points indicated on L-LPD curves are the values calculated by the crack analysis method mentioned in section 3.1 using the calculated poly-linear TSD as a constitutive equation. The observed L-LPD curve and the calculated points agree well, so this inverse analysis method is considered to be an appropriate method for calculating TSD.

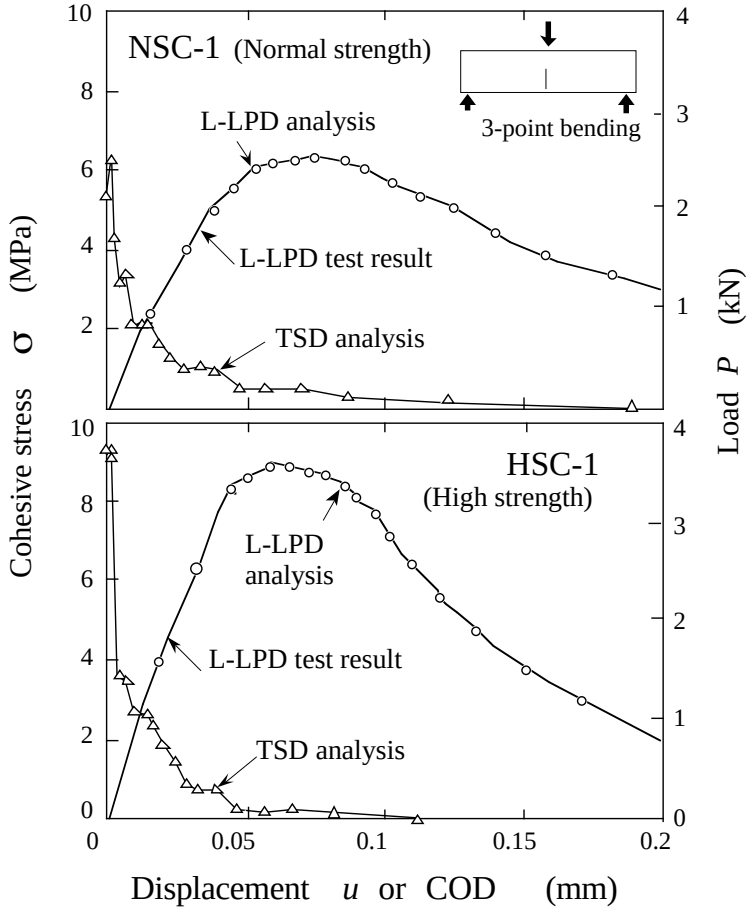

Figure 4. Load - load point displacement (L-LPD) curve and analyzed TSD

3 EFFECT OF HEATING ON THE FRACTURE PROPERTIES OF CONCRETE

3.1 Outline of experiment

Tables 1 and 2 give the materials and designed mixture proportions, respectively. Ordinary portland cement was used with water-cement ratios (W/C) of 0.5. Maximum aggregate size (Gmax) was changed as 5 mm for mortar and 10 mm for concrete. Table 3 gives the test factors and levels. The temperature condition was in two levels: 20 and 60℃. Test period was 0, 4, 13 weeks.

Table 1. Materials used for the experiment

Materials	Mark	Detail
Cement	C	Ordinary portland cement, Gravity=3.16g/cm^3
Fine aggregate	S1	Pit sand, Specific gravity=2.50 g/cm^3 Absorption=2.45%, F.M.=2.12
	S2	Crushed sand, Specific gravity=2.64g/cm^3, Absorption=1.23% F.M=3.01
Coarse aggregate	G	Crushed stone, Specific gravity=2.66g/cm^3, Absorption=0.97% Absolute volume=59.5%, Gmax=10mm
Admixture	Ad	Air entraining and water reducing agent

Table 2. Designed mixture proportions

	W/C (%)	Gmax (mm)	Air (%)	S/a (%)	W (kg/m^3)	C (kg/m^3)	S1 (kg/m^3)	S2 (kg/m^3)	G (kg/m^3)	Ad (%)
Mortar	50	5	-	100	283	566	403	994	-	-
Concrete	50	10	4.5	45	180	360	223	550	967	Cx0.25

Table 3. Factors and levels

Factors	Levels
Specimen	Mortar, Concrete
Test temperature (℃)	20, 60
Test period after 24 days water curing (week)	0, 4, 13

After the 28-day water curing at 20℃, specimens were cured in two temperature conditions of 20℃ and 60℃ for 4 and 13 weeks in 60%RH. After the curing, three-point bending tests were conducted to measure the load versus crack mouth opening displacement (L-CMOD) curves. Test conditions follow the JCI Standard(JCI-S-001-2003).Specimen size was 40mm x 40 mm x 160 mm. The span length was 120 mm, and notch length was 12mm. A servo-controlled hydraulic tester having a closed loop system (manufactured by MTS) was used to achieve accurate measurement of the load-displacement curves. Specimen was attached to a loading machine and loaded with constant CMOD speed. Sensitive clip gauges for displacement control (MTS-632.02) were used for the CMOD measurement. Test set up is shown in Fig. 5.

The tension softening diagram was determined by poly-linear approximation analysis method based on the obtained load-CMOD curves. Fracture parameters, such as fracture energy and cohesive strength were evaluated from the obtained tension softening diagram. After the bending tests, compressive strength was measured.

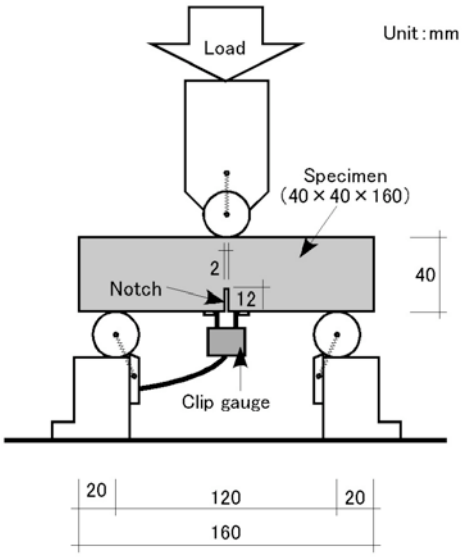

Figure. 5. Three-point bending test for center notched concrete beam

3.2Test results and discussions

Fig. 6 shows the results of compression tests of concrete and mortar. The compressive strength of the both concrete and mortar subjected heating of 60℃ tends to be lower than those of 20℃ at the curing period of 4 weeks and 13 weeks. Fig. 7 shows typical load- crack mouth opening displacement (L-CMOD) curves of the specimens. Stable load displacement curves were obtained for all tests.

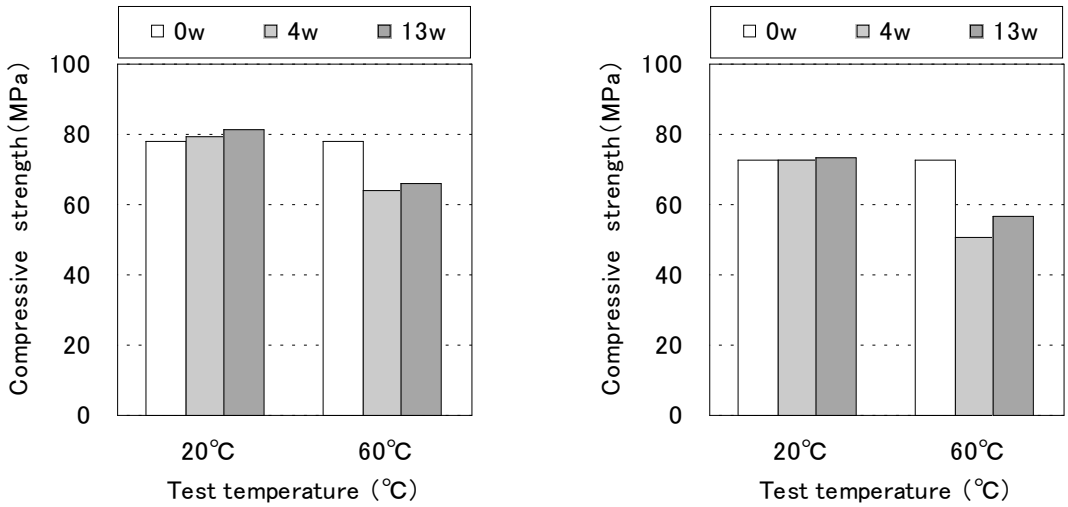

(a) Concrete (b) Mortar

Figure 6. Compressive strength

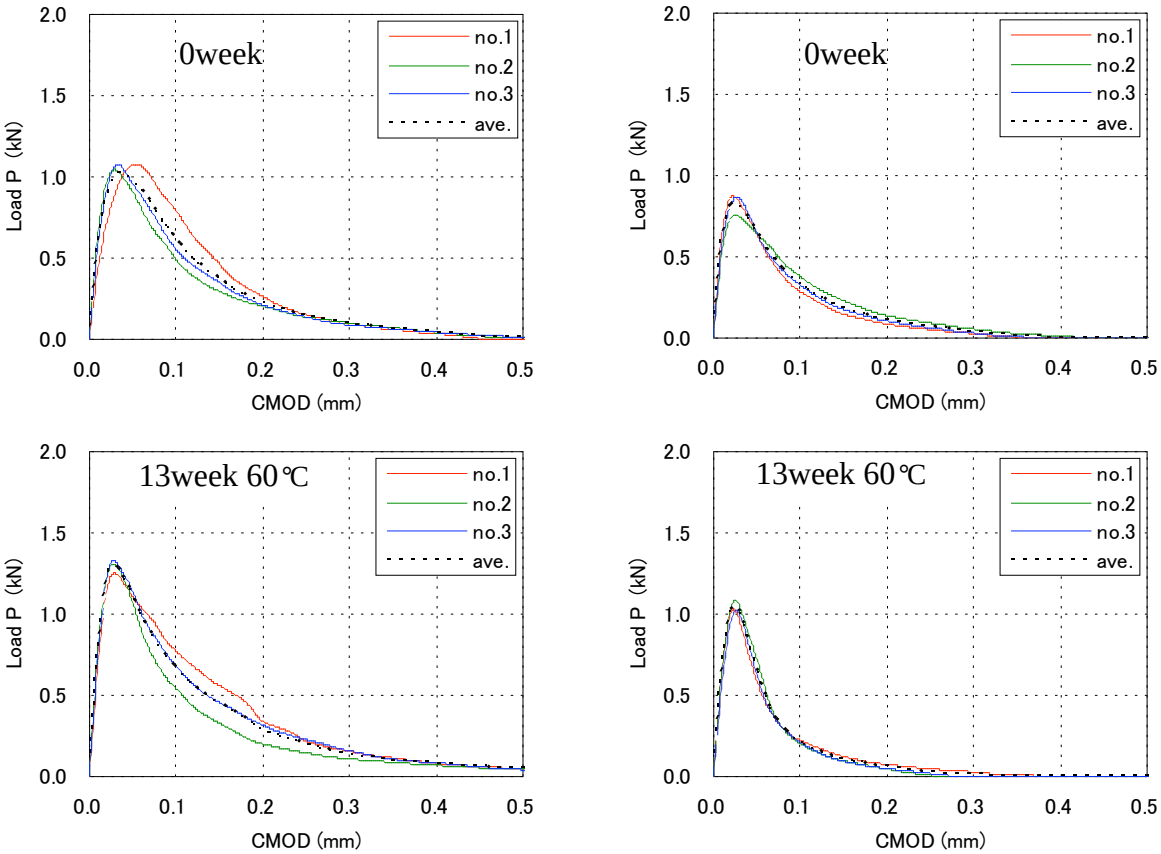

(a) Concrete (b) Mortar

Figure 7. Typical load – crack mouth opening displacement (L-CMOD) curve

Fig. 8 and 9 shows the tension softening diagram (TSD) analyzed from observed L-CMOD of concrete and mortar respectively. Fig. 10 shows fracture energy *G*FTSD which were calculated from the surrounded area

of TSD. Fracture energy of concrete (Gmax=10mm) is higher than that of the mortar (Gmax=5mm). This is because the fracture process zone of the concrete specimen becomes large due to the crack deflection effect of the aggregate, thus an energy dissipation becomes higher than that of the mortar specimen. In case of concrete, fracture energy is not significantly changed at the curing conditions of 20℃ and 60℃. Contrary to this, mortar specimen cured at 60℃ for 90days tend to develop a low fracture energy than those cured at 20℃ for 90days and showed brittle behavior. This is because the micro crack of paste matrix becomes high with the increase of curing temperature. This means that the aggregate size is an important to retain fracture toughness of concrete in the condition of high temperature.

20℃ 60℃

Figure 8. Tension softening diagram (concrete, Gmax=10mm)

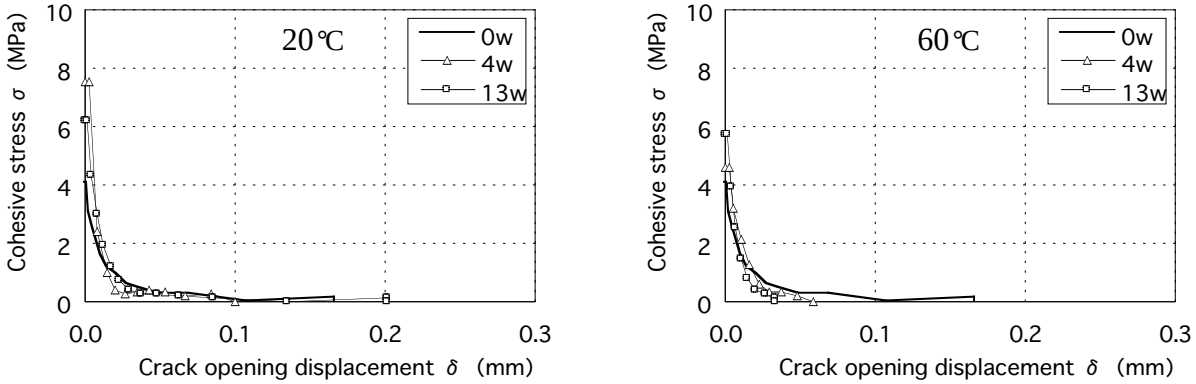

Figure 9. Tension softening diagram (mortar, Gmax=5mm)

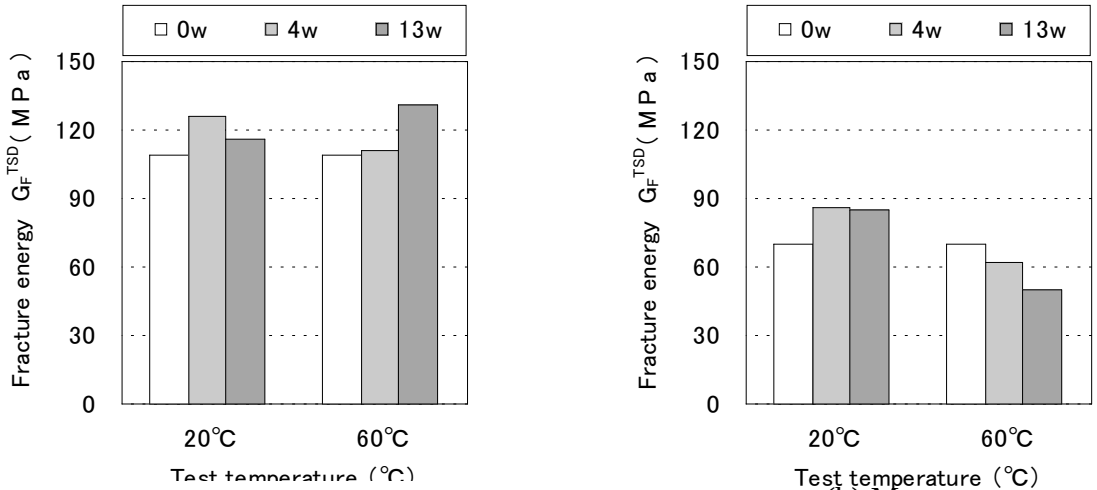

(a) Concrete (b) Mortar

Figure 10. Fracture enrgy

4. CONCLUSIONS

1) Poly-linear tension softening inverse analysis method was introduced. In this method, the complete tension softening diagram can be obtained from one load-displacement curve.
2) Specimens cured at 60℃ for 90days tend to show low compressive strength than those cured at 20℃ for 90days.
3) Specimen of maximum aggregate size 10 mm tends to show high energy consumption to compare with specimen of maximum aggregate size 5 mm.
4) Specimens of maximum aggregate size 5 mm cured at 60℃ for 90days tend to show low fracture energy than those cured at 20℃ for 90days.

REFERENCES

Cotterell, B., Paramasivam, P. and Lam, K. Y. 1992. Modelling the fracture of cementitious materials. Materials and Structures. Vol 25:145. P 14-20.

Foote, R., Mai, Y. W. and Cotterell, B. 1986. Crack growth resistance curves in strain-softening materials. J. of Mech. Physics of Solids. Vol. 34:6. P 593-607.

Gopalaratnam, V. S. and Shah, S. P., 1985. Softening response of plain concrete in direct tension. ACI Journal. May-June. P 310-323.

Hillerborg, A., Modeer, M. and Petersson, P. E. 1976. Analysis of crack formation and crack growth in concrete by means of fracture mechanics and finite elements. Cement and Concrete Research. Vol. 6:6. P 773-782.

JCI Standard 2003. Method of test for fracture energy of concrete by use of notched beam. JCI-S-001-2003. Japan Concrete Institute (JCI).

Kitsutaka,Y., Kamimura,K. and Nakamura, S. 1994. Evaluation of aggregate properties on tension softening behavior of high strength concrete. High Performance Concrete. American Concrete Institute. ACI SP 149-40. P 711-727. 2003. Method of test

Kitsutaka, Y. 1997. Fracture parameters by polylinear tension-softening analysis. J. Engrg. Mech., ASCE. Vol. 123:5. P 444-450.

Li, V. C., Chan, C. M. and Leung, C. K. Y. 1987. Experimental determination of the tension softening relations for cementitious composites. Cement and Concrete Research. Vol. 17:3. P 441-452.

LLorca, J. and Elices, M., (1990). A simplified model to study fracture behavior in cohesive materials. Cement and Concrete Research. Vol. 20:1. P 92-102.

Roelfstra, P. E. and Wittmann, F. H. 1986. Numerical method to link strain softening with failure of concrete Fracture Toughness and Fracture Energy of Concrete. Elsevier Science Publishers. F. H.Wittmann ed. P 163-175.

Tada, H., Paris, P. C. and Irwin, G. R. 1985. The stress analysis of cracks handbook. Second edition. Paris Productions Incorporated. Appendix B. 2-16. 2-27.

Wang, Y., Li, V. C. and Backer, S. 1990. Experimental determination of tensile behavior of fiber reinforced concrete. ACI J. Vol. 87:5. P 461-468.